On the physical mechanisms governing self-excited pressure surge in Francis turbines

A Müller[1], A Favrel[1], C Landry[1], K Yamamoto[1] and F Avellan[1]

[1] EPFL Laboratory for Hydraulic Machines, Av. de Cour 33 Bis, 1007 Lausanne, Switzerland

E-mail: andres.mueller@epfl.ch

Abstract. The required operating range for hydraulic machines is continually extended in an effort to integrate renewable energy sources with unsteady power outputs into the existing electrical grid. The off-design operation however brings forth unfavorable flow patterns in the machine, causing dynamic problems involving cavitation, which may represent a limiting factor to the energy production. In Francis turbines it is observed that the self-excited oscillation of a vortex rope in the draft tube cone prevents the delivery of maximum power when required. This phenomenon is referred to as full load pressure surge and has been the object of extensive research during the past decades. Several contributions deepened its understanding through measurement and simulation of the local flow properties and the global stability parameters. The draft tube pressure level and the runner outlet swirl are identified as key variables in the modelling of the vortex rope dynamics. Recently, a cyclic appearance of blade cavitation has been observed at overload conditions in a multiphase numerical simulation coupling the runner and the draft tube. From the analysis of the simulation it becomes obvious that the cyclic appearance of blade cavitation has a direct effect on the runner outlet swirl, thus introducing an additional interaction mechanism that is not accounted for in formerly published models. For the presented work, the results of this numerical study are confirmed experimentally on a reduced scale model of a Francis turbine. Several wall pressure measurements in the draft tube cone are performed, together with high speed visualizations of the vortex rope and the blade cavitation. The flow swirl is calculated based on Laser Doppler Velocimetry measurements. A possible mechanism explaining the coupling between the self-excited pressure and vortex rope oscillation and the cyclic appearance of the blade cavitation is proposed. Furthermore, the streamwise propagation speed of the flow swirl in the draft tube is calculated. The results offer important insights in the physics of high load pressure surge and contribute to the further development of numerical draft tube flow and stability models.

1. Introduction

Pressure oscillations in hydraulic machines have been known to critically disturb the operation of hydropower plants since the early nineteen-hundreds [1]. The physical properties of this occurrence depend on the load range. At flow rates larger than the nominal value at the best efficiency point of the turbine, an axisymmetrically shaped cavitation volume is formed in the draft tube attached to the runner hub. This cavity or vortex rope may start to oscillate and enter a self-excited regime, accompanied by violent pressure pulsations throughout the hydraulic system. The physical mechanisms leading to its onset are not yet conclusively identified. The off-design operation of hydraulic machines plays an increasingly important role in guaranteeing the electrical grid stability during the integration of renewable energy sources. It is therefore crucial to understand, model, predict and eventually prevent such an unstable behavior.

The stability of the system may be analyzed by using one-dimensional, hydroacoustic models of the draft tube flow. Different approaches in terms of defining the main model parameters and thus identifying the dominant destabilizing mechanisms are discussed by Nicolet [2], Koutnik *et al.* [3], Alligné *et al.* [4, 5, 6] and Dörfler *et al.* [7, 8, 9]. Recent contributions to the analytical description of the two-phase flow are made by Kuibin *et al.* [10, 11] and Susan-Resiga *et al.* [12]. Furthermore, self-excited pressure oscillations are successfully reproduced by CFD calculations for selected test cases by Chirkov *et al.* [13] and Braun *et al.* [14].

Experimentally, the unsteady, two-phase flow in the draft tube cone of a reduced scale model of a Francis turbine has been characterized by means of wall pressure synchronized Laser Doppler velocimetry (LDV) and fluorescent particle image velocimetry (PIV) measurements [15, 16]. In parallel, the results of a multi-phase numerical simulation coupling the runner and the draft tube of the same test case suggest the existence of cyclically appearing blade cavitation, responsible for a sudden swirl breakdown in the flow leaving the runner [14]. In order to confirm the findings from the CFD calculation, high-speed visualizations of the runner blade channels are performed in the frame of the present work. Furthermore, the flow swirl is calculated based on the LDV measurements at two streamwise positions in the draft tube cone. An important mechanism governing the self-excited pressure oscillations on the investigated machine is thereby revealed and discussed.

2. Experimental setup and methodology

A 1:16 reduced scale model of a Francis turbine is installed on the EPFL test rig PF3 of the Laboratory of Hydraulic Machines, as shown in figure 1. The prototype of the generating unit features a nominal power of 444 MW and is located in the Canadian province of British Columbia. The test rig is operated in a closed-loop configuration, with two axial double-volute pumps generating the specified head. The discharge is adjusted with the guide vane opening and the pressure level in the draft tube is set by a vacuum pump in the downstream reservoir.

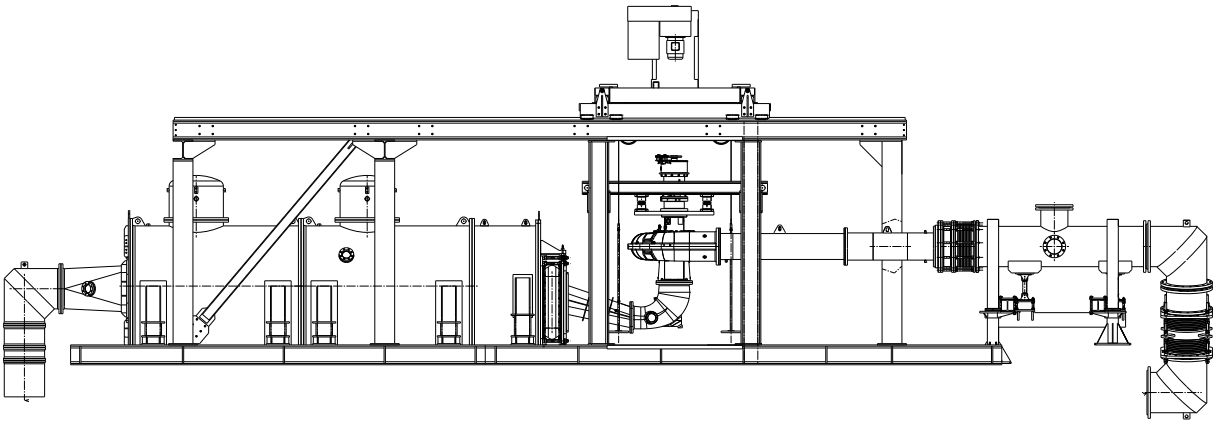

Figure 1: Reduced scale physical model of a Francis turbine installed on EPFL test rig PF3.

A total of 28 piezo-resistive pressure sensors are installed throughout the system, of which 2×4 are located in the Plexiglas cone, uniformly distributed on the circumference of the two LDV measurement sections. The setup for the pressure synchronized velocity measurements is shown in figure 2. Section 1 and Section 2 are located $0.39 \times D_{\bar{1}}$ and $1.02 \times D_{\bar{1}}$ downstream of the runner outlet, respectively, where $D_{\bar{1}}$ is the outer runner outlet diameter. The axial and tangential velocity components Cm and Cu are measured with a factory aligned state of the

art LDV probe in non-coincidence mode, mounted on a 2-D traversing system for displacements along the x and z axes.

The LDV measurements are performed at 20 radial positions along the x-axis between the cone wall and the cone center in Section 1, and 21 radial positions in Section 2. Each LDV measurement is synchronized with the acquisition of a reference wall pressure signal at the given cross-section. The latter is then used to calculate a mean phase average of the velocity components with the method introduced in [15], based on the instantaneous phase angle of an analytic signal of the reference pressure containing its Hilbert transform [17]. The result is an averaged evolution of Cm and Cu during a mean period of the pressure oscillation at each radial position. The pressure factor c_p is the fluctuating part of the wall pressure p divided by the specific energy and the water density.

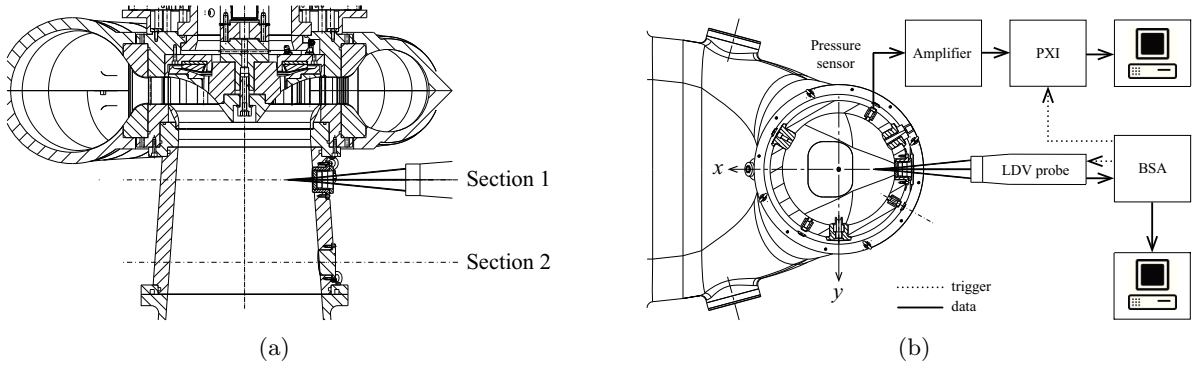

Figure 2: Streamwise sections (left) and acquisition chain (right) for the LDV measurements. The PXI is the modular electronic instrumentation platform used for the pressure data acquisition and the BSA (burst spectrum analyzer) determines the velocity components from the LDV probe.

The cavitation on the runner blades is visualized using a high speed camera. In order to minimize the optical distortion, a water filled window is glued to the exterior cone wall, as shown in figure 3. The runner outlet is illuminated from below with a stroboscopic light source, which is synchronized with the high speed camera. The strobe frequency is set to $8 \times n$, where n is the runner frequency. Hence, at a total number of 16 blades, a picture frame is recorded of every other blade passing in front of the lens.

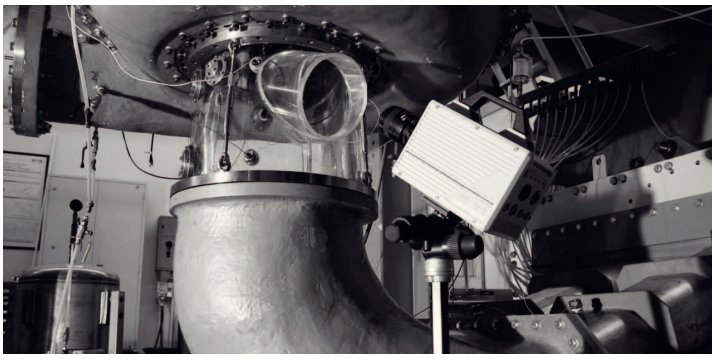

Figure 3: Picture of the flow visualization setup with high speed camera and inclined water filled Plexiglas window.

3. Operating conditions and vortex rope oscillation

Table 1 summarizes the operating conditions at which the presented measurements are performed. The displayed values represent an average, since minor fluctuations of the test conditions naturally occur. The dimensionless n_{ED} and Q_{ED} are the speed and discharge factors (defined in the nomenclature), σ is the cavitation number, N is the number of runner revolutions per minute.

Table 1: Summary of the operating conditions.

n_{ED} (-)	Q_{ED} (-)	σ (-)	N (min^{-1})	H (m)	$Q_{\mathrm{ED}}/Q_{\mathrm{ED,BEP}}$ (-)
0.288	0.259	0.11	800	26.8	1.3

In order to illustrate the oscillation of the vortex rope at the given operating conditions, a high speed visualization of the draft tube flow is performed. Images at 10 equally spaced moments over a period of the wall pressure fluctuation are shown in figure 4. The corresponding raw wall pressure signal in the measurement section 1 is shown in figure 5, where the vertical dashed lines represent the instants at which the frames in figure 4 are recorded.

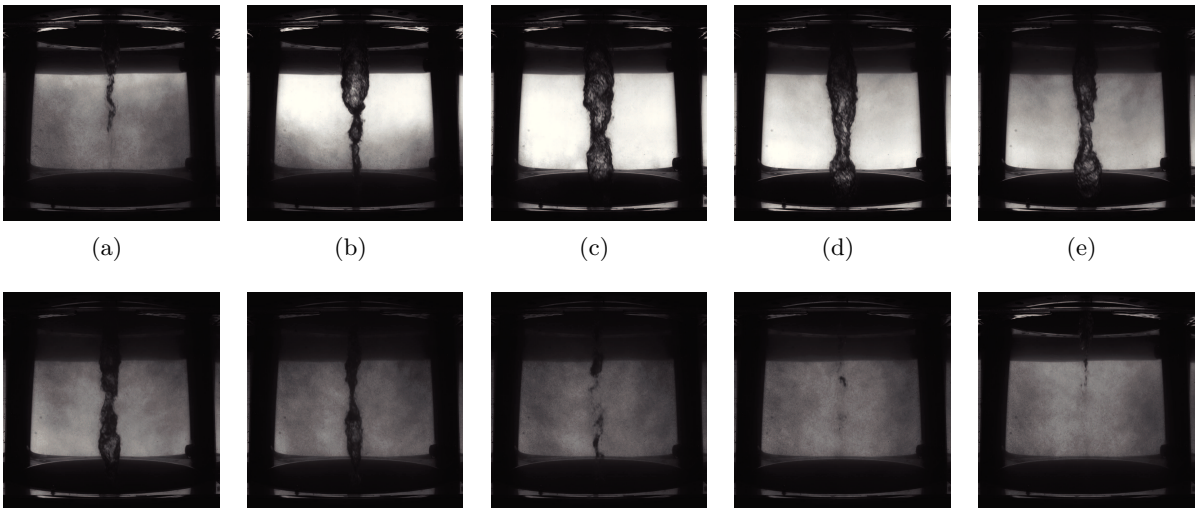

Figure 4: High speed visualization of the vortex rope oscillation in the draft tube cone.

The good contrast between the liquid and gaseous phase is obtained by using a highly uniform LED backlight source. The cavity at this operating point is rather slender, compared to the one observed at lower values of the speed factor n_{ED}. High structural vibrations of the test rig accompany the self-oscillation and the vortex rope is characterized by a swift and complete collapse, before rebuilding again.

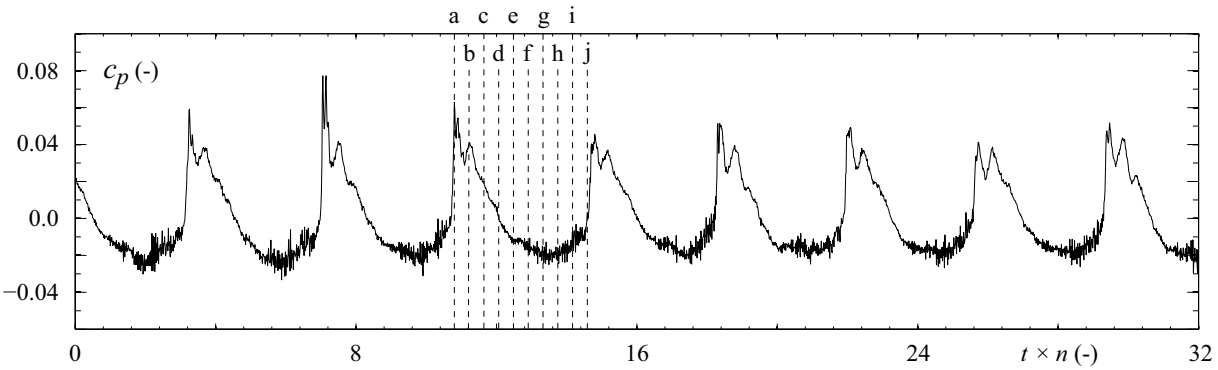

Figure 5: Wall pressure factor c_p as a function of the number of runner revolutions. Images of the vortex rope taken at (a) ... (j) are shown in figure 4.

4. Observation of cyclic blade cavitation appearance

The visualization of the interblade channel flow with the setup described in Section 2 shows periodically appearing cavitation around the trailing edges of the blades, as predicted by numerical simulation [14]. This is illustrated in figure 6 for 15 uniformly distributed instants over one period of the pressure oscillation. The roman numbering refers to the corresponding locations in the reference wall pressure signal in figure 7.

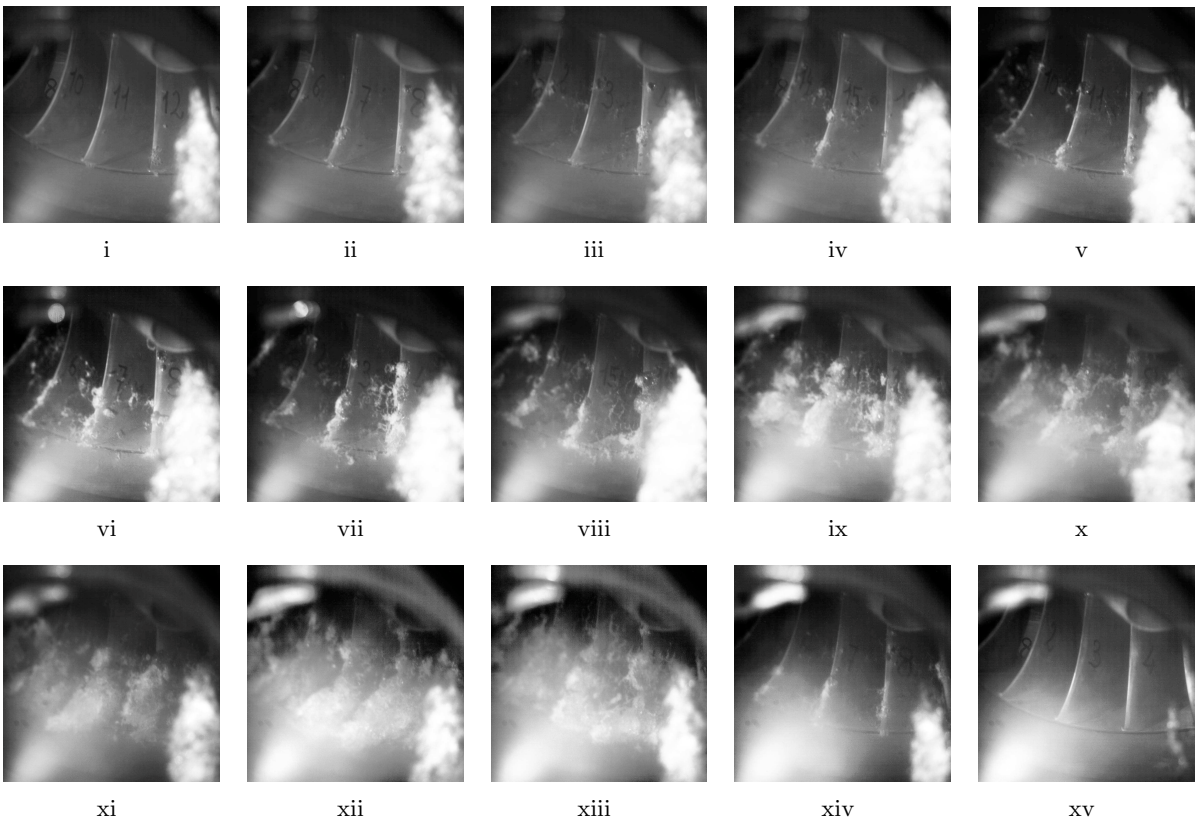

Figure 6: Cavitation on the runner blades during one period of the pressure oscillation.

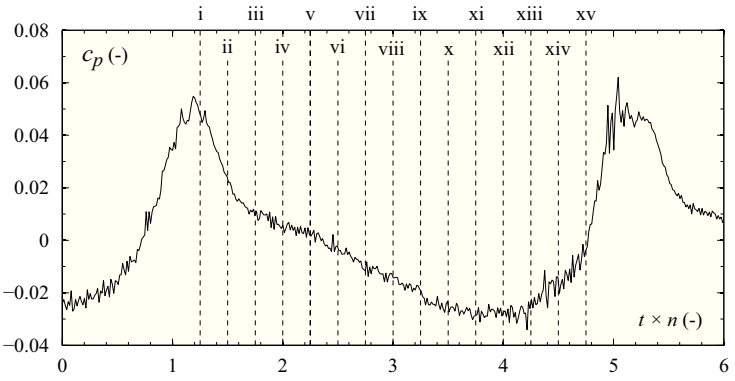

Figure 7: Fraction of the wall pressure factor signal c_p including one complete cycle, as a function of the number of runner revolutions. The instants corresponding to the pictures in figure 6 are shown as vertical dashed lines.

5. Flow swirl variation

The flow swirl is defined as the ratio of the axial flux of the angular momentum and the axial flux of the axial momentum [18]. Based on the tangential and axial velocity components Cu and Cm obtained from the LDV measurements and assuming axisymmetry, the swirl number on both the measurement sections shown in figure 2(a) can be calculated according to

$$S = \frac{\int_0^R r^2 \cdot Cu \cdot Cm \, \mathrm{d}r}{R_{\bar{1}} \cdot \int_0^R r \cdot Cm^2 \, \mathrm{d}r} \,, \tag{1}$$

where $R_{\bar{1}}$ is the external runner outlet diameter and r the radial measurement position. The result is shown in figure 8, together with the mean phase averaged wall pressure factor in the respective measurement section.

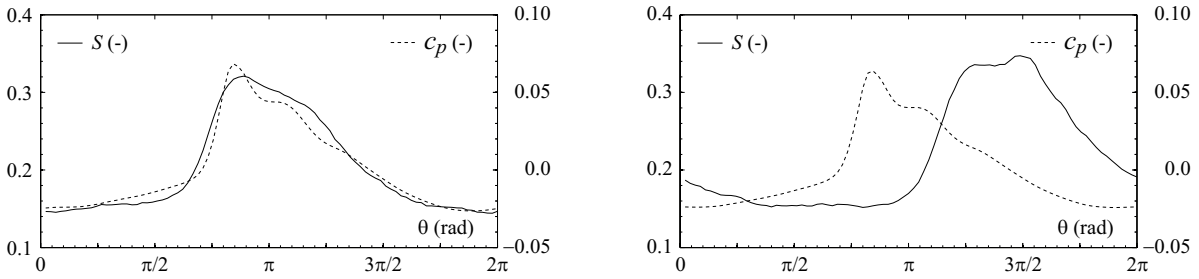

(a) Section 1

(b) Section 2

Figure 8: Pressure phase averaged swirl number S together with wall pressure factor c_p. The interval $[0, 2\pi]$ represents one mean period of the wall pressure oscillation.

Figure 8(a) displays a significant increase in the swirl number in Section 1, almost synchronously with the rise in the mean phase averaged wall pressure factor c_p. A similar behavior is observed in Section 2, with a delay of roughly $2\pi/5$ or 20% of the period compared to the swirl peak in Section 1. The mean pressure oscillation period in Section 2 is $\bar{T} = 0.595$ s, averaged across all the measurements corresponding each to a radial LDV position. Hence, with a vertical distance of 0.22 m between the two measurement sections, this results in an axial propagation speed of 1.85 $\mathrm{m \cdot s^{-1}}$. The mean discharge speed in Section 2 is 4.12 $\mathrm{m \cdot s^{-1}}$, based on the discharge in the test rig measured by an electromagnetic flow meter. The swirl is hence propagating in streamwise direction at 44% of the mean axial flow velocity.

6. Summary and discussion

The noisy section of the wall pressure signal between the moments (e) and (j) in figure 5 is caused by the significant presence of bubbles in the surrounding flow, observable in figure 4. The visualization of the flow leaving the runner in figure 6 strongly suggests that these bubbles originate from the cavitation on the runner blades. The moment the bubbles disappear from the flow, when the image background starts clearing up from above in figure 4(a), corresponds to the wall pressure peak.

The formation and collapse of the cavitation on the runner blades in figure 6 is periodic and regular. The current setup does however not allow a quantification of its appearance, for instance by calculating the volume through image processing as for the vortex rope in the draft tube cone [19]. It is therefore difficult to establish a phase relationship with the pressure signal and hence to accurately determine the role played by the blade cavitation in the flow swirl variation. It is noted that at the instant (xv) in figure 7, corresponding to the situation shown in figure 6xv and situated exactly at the end of the noisy part and the onset of the abrupt pressure rise, the cavitation on the runner blades has completely disappeared together with the vortex rope in the lower right corner of the image.

The link between the vortex rope and the blade cavitation oscillation appears to be established through the flow swirl. The formation of cavitation on the runner blades is likely to cause a reduction of the relative flow angle β at the runner outlet and hence a loss of the swirl. During this phase, the cavitation continuously detaches from the runner blades and is evacuated in form of small bubbles injected into the draft tube flow. At some point, the blade cavitation collapses entirely, possibly due to a pressure rise following the deceleration of the fluid. This leads to a sudden reestablishment of the flow swirl, inducing a rise in the cone wall pressure and hence a pressure drop in the cone center, leading to a redevelopment of the vortex rope. The vortex rope seems to reach its maximum shortly after the pressure peaks, during the "clear" phase of the flow, sees its volume reduced during the "bubbly" phase and then collapses together with the blade cavitation.

7. Conclusions and perspectives

In order to identify the key physical mechanisms involved in full load pressure surge, a series of experiments are conducted on a reduced scale physical model of a Francis turbine. Flow visualizations of the vortex rope and the cavitation on the runner blades are presented together with reference wall pressure signals. LDV measurements on two streamwise positions in the draft tube cone are used to establish the pressure phase averaged axial and tangential velocity profiles along the radius of the given cross-section. The knowledge of the velocity profiles at a specified number of time steps over on mean period then enables the calculation of the instant flow swirl number.

Based on the analysis of the wall pressure synchronized flow visualizations and the swirl number, a potential governing mechanism is proposed, identifying the swirl variation due to the development of cavitation on the runner blades as key actor. It is however not necessarily obvious how the roles are distributed between the vortex rope and blade cavitation, or in other words what exactly provokes the onset of the self-excited pressure oscillation. Further investigations need to be performed around a critical point near the stability limit, featuring a stable vortex rope, in order to clarify how the two phenomena evolve during the passage from a stable to an unstable configuration.

Finally, the described mechanism suggests an important role of the runner geometry in the occurrence of full load pressure surge in the presented test case, defining to what extend cavitation on the runner blades is likely to develop at off-design operating conditions.

Acknowledgments
The research leading to the results published in this paper is part of the HYPERBOLE research project, granted by the European Commission (ERC/FP7- ENERGY-2013-1-Grant 608532). The authors would also like to thank the EOS Holding for their financial support and BC Hydro for making available the reduced scale model, in particular Danny Burggraeve and Jacob Iosfin. Moreover, the authors would like to acknowledge the commitment of the Laboratory for Hydraulic Machines' technical staff, especially Georges Crittin, Maxime Raton, Alain Renaud and Vincent Berruex.

Nomenclature

Cm	axial velocity component	$(\mathrm{m{\cdot}s^{-1}})$	n	runner frequency	(Hz)
Cu	tangential velocity component	$(\mathrm{m{\cdot}s^{-1}})$	n_{ED}	$= (n \cdot D)/\sqrt{E}$	(-)
c_p	$= (p - \bar{p})/(\rho E)$	(-)	p	pressure	(Pa)
D	runner diameter	(m)	Q_{ED}	$= Q/(D^2 \cdot \sqrt{E})$	(-)
E	specific energy; $E = gH$	$(\mathrm{J{\cdot}kg^{-1}})$	R	runner radius	(m)
g	gravitational acceleration	$(\mathrm{m{\cdot}s^{-2}})$	S	swirl number	(-)
H	head	(m)	ρ	density	$(\mathrm{kg{\cdot}m^{-3}})$
N	runner speed	$(\mathrm{min^{-1}})$	σ	cavitation number	(-)

References

[1] Rheingans W 1940 *Transactions of the ASME* **62** 171–184
[2] Nicolet C 2007 *Hydroacoustic Modelling and Numerical Simulation of Unsteady Operation of Hydroelectric Systems* Ph.D. thesis no. 3751, Ecole polytechnique fédérale de Lausanne, Switzerland
[3] Koutnik J, Nicolet C, Schohl G A and Avellan F 2006 *Proc. of the 23th IAHR Symposium on Hydraulic Machinery and Systems, Yokohama, Japan*
[4] Alligné S, Maruzewski P, Dinh T, Wang B, Fedorov A, Iosfin J and Avellan F 2010 *IOP Conference Series: Earth and Environmental Science* vol 12 (IOP Publishing) p 012025
[5] Alligné S 2011 *Forced and Self Oscillations of Hydraulic Systems Induced by Cavitation Vortex Rope of Francis Turbines* Ph.D. thesis no. 5117, Ecole polytechnique fédérale de Lausanne, Switzerland
[6] Alligné S, Nicolet C, Tsujimoto Y and Avellan F 2014 *Journal of Hydraulic Research* ahead–of–print
[7] Dörfler P 2009 *Proceedings of the 3rd Meeting IAHR Workgroup on Cavitation and Dynamic Problems in Hydraulic Machinery and Systems, Brno*
[8] Dörfler P, Keller M and Braun O 2010 *IOP Conference Series: Earth and Environmental Science* vol 12 (IOP Publishing) p 012026
[9] Dörfler P, Braun O and Tsujimoto Y 2011 *Proceedings of the WIMRC 3rd International Cavitation Forum, University of Warwick, UK*
[10] Kuibin P, Okulov V, Susan-Resiga R and Muntean S 2010 *IOP Conference Series: Earth and Environmental Science* vol 12 (IOP Publishing) p 012051
[11] Kuibin P, Pylev I and Zakharov A 2012 *IOP Conference Series: Earth and Environmental Science* vol 15 (IOP Publishing) p 022001
[12] Susan-Resiga R, Muntean S, Avellan F and Anton I 2011 *Applied Mathematical Modelling* **35** 4759–4773
[13] Chirkov D, Avdyushenko A, Panov L, Bannikov D, Cherny S, Skorospelov V and Pylev I 2012 *IOP Conference Series: Earth and Environmental Science* vol 15 (IOP Publishing) p 032038
[14] Braun O, Taruffi A, Ruchonnet N, Müller A and Avellan F 2013 *Proc. of the 5th Int. Meet. on Cavitation and Dynamic Problems in Hydraulic Machinery and Systems, Lausanne, Switzerland*
[15] Müller A, Bullani A, Dreyer M, Roth S, Favrel A, Landry C and Avellan F 2012 *IOP Conference Series: Earth and Environmental Science* vol 15 (IOP Publishing) p 032040
[16] Müller A, Dreyer M, Andreini N and Avellan F 2013 *Experiments in Fluids* **54** 1–11
[17] Bendat J S and Piersol A G 2010 *Random data: Analysis and measurement procedures* 4th ed (Wiley)
[18] Gupta A K, Lilley D G and Syred N 1984 *Swirl Flows* (Abacus Press, UK)
[19] Müller A 2014 *Physical Mechanisms governing Self-Excited Pressure Oscillations in Francis Turbines* Ph.D. thesis no. 6206, Ecole polytechnique fédérale de Lausanne, Switzerland